NASA CR-165828

ERROR NORMS FOR THE ADAPTIVE SOLUTION OF THE NAVIER-STOKES EQUATIONS

C. K. Forester

Boeing Military Airplane Company
Seattle, Washington

Prepared for
Langley Research Center
under contract NAS1-16408

NASA

National Aeronautics and
Space Administration

Langley Research Center
Hampton, Virginia 23665

May 1982

NF01354

1 Report No	2 Government Accession No	3 Recipient's Catalog No
NASA CR 165828		

4 Title and Subtitle	5 Report Date
Error Norms for the Adaptive Solution of the Navier-Stokes Equations	July 1982
	6 Performing Organization Code

7 Author(s)	8 Performing Organization Report No
C. K. Forester	
	10 Work Unit No

9 Performing Organization Name and Address	
Boeing Military Airplane Company P.O. Box 3707 Seattle, Washington 98124	11 Contract or Grant No NAS1-16408
	13 Type of Report and Period Covered

12 Sponsoring Agency Name and Address	
National Aeronautics and Space Administration Washington, D.C. 20546	Contractor Report
	14 Sponsoring Agency Code

15 Supplementary Notes
Final Report

16 Abstract

The adaptive solution of the Navier-Stokes equations depends upon the successful interaction of three key elements; 1) the ability to flexibly select grid length scales in composite grids, 2) the ability to efficiently control residual error in composite grids, and 3) the ability to define reliable, convenient error norms to guide the grid adjustment and optimize the residual levels relative to the local truncation errors. An initial investigation was conducted to explore how to approach developing these key elements. Conventional error assessment methods were defined and defect- and deferred-correction methods were surveyed. The one-dimensional potential equation was used as a multi-grid test-bed to investigate how to achieve successful interaction of these three key elements. Recommendations are made for further work on error norms and enhanced residual error control for the potential and Navier-Stokes equations in a series of computer codes of increasing complexity. Culmination of this effort is for nested multi-grid modeling of flows with singularities or steep gradients.

17 Key Words (Suggested by Author(s))	18 Distribution Statement
Partial Differential Equations Navier-Stokes Equations Numerical Solution Methods Numerical Error Assessment Multi-grid and Defect Corrections	

19 Security Classif (of this report)	20 Security Classif (of this page)	21 No of Pages	22 Price*
Unclassified	Unclassified		

NASA-C-168 (Rev 10-75)

N82-32637#

ERROR NORMS FOR THE ADAPTIVE SOLUTION
OF THE NAVIER-STOKES EQUATIONS

C. K. Forester

Boeing Military Airplane Company
Seattle, Washington 98124

for

NASA Langley Research Center
Hampton, Virginia

TABLE OF CONTENTS

TABLE OF CONTENTS (concluded)

NOMENCLATURE

A	Channel cross-sectional area, 1-D test problem
CPU	Computer processor unit
E	Error norm
L	Differential operator of PDE system, length of channel for 1-D test problem
PDE	Partial differential equation
U	Dependent variable vector of PDE system
ϕ	Dependent variable
VL	Volume of computational cell, 1-D test problem
W	Cartesian velocity component
We	Cartesian velocity component at domain entrance
y	Cartesian coordinate normal to flow direction, time-like coordinate
z,Z	Cartesian coordinate in flow direction
I_I^{I+1}	Prolongation operator for coarse-to-fine grid interpolation
I_{I+1}^{I}	Restriction operator for fine-to-coarse grid interpolation
I	Grid index, positive integer
Ig	'Goal grid' index value of superscript I
R^I	Local residual error on grid I
RS^I	Source term for defect correction
T^I	Local truncation error on grid I
u^I	Unknown variables on grid I, an error term is associated with each value
u^{Ig}	Certified values of dependent variable vector on 'goal grid'
M	Integer for identifying the cell location in grid I, positive integer
M_{max}	Number of cells in the analysis domain

LIST OF FIGURES

1.0 SUMMARY

The current practice for applied analysis in the aerospace industry is to use specially selected combinations of coupled zonal models - inviscid, shear layer, etc. - to approximate the field equations of fluid mechanics for various applications. The zonal models involve systems of ordinary and partial differential equations (field equations). These equations are simulated with numerical methods which possess two types of numerical errors - residual errors and truncation errors. Residual (solution process) errors arise due to insufficient iterations of implicit algebraic equations by relaxation or the inversion of ill-conditioned matrices. Truncation (grid related) errors arise due to the selection of the grid, the grid-related algebraic equations and the associated boundary and initial conditions. Residual errors and truncation errors can be very significant. Assessing the effects of numerical error on the modeling of the field equations is a tedious and expensive process involving parametric cycling through various tolerances on residual error and various grid densities and distributions. Grid length-scale control to properly resolve shock and shear layer singularities is unavailable except for specialized cases. Because of these difficulties, numerical error effects are not commonly examined or controlled with precision using conventional methods of numerical analysis, and this can lead to a misinterpretation of computed results.

Efficient solution of the equations of fluid mechanics requires the availability of adaptive mesh generation and numerical error assessment methods to define numerical errors and guide the grid adjustment process. The overall goal of this research program is the development of these methods.

The objectives of the work reported herein were to begin development of algorithms to define error norms (for use as resolution monitors) for numerical solution of PDE's and to begin development of a multi-level adaptive grid technique for application to the solution of the various equation sets used to model fluid flow. The present work is an initial exploratory investigation of resolution monitors and adaptive grid technology.

The approach was as follows. The literature on error assessment and multi-grid methods was briefly reviewed. From this, conventional error assessment methods were defined and are briefly described. Three variable-order-accuracy defect-correction approaches were identified. The one-dimensional (1-D) incompressible potential equation was selected as a test bed to investigate error assessment and multi-grid methods. A test problem, a channel with a constriction, was selected for which analytic solutions were available. The equation was solved for the test problem using point relaxation for a range of mesh densities and distributions and the various error assessment techniques were evaluated. The test problem was also solved using point relaxation and a multi-grid scheme and the characteristics of the multi-grid method were evaluated.

One result is that multi-grid schemes are promising as a basis for developing resolution monitors and adaptive grid techniques. Brandt's methodology appears to be the most suitable approach to adaptive-grid-control. The present study suggests that the multi-grid technology is conceptually straightforward to apply to conventional computer codes which solve elliptic problems. A second is that for the test problem, reliable estimates of the maximum global error were obtained from solution output for a number of grid levels. From the work completed, it is expected that substantial improvements are possible for assessing and controlling numerical errors. A third result is that significant improvement for efficient residual error control was demonstrated with the test problem. Further work is, however, required to develop the three key elements: (1) error norms to guide grid adjustment for truncation error control, (2) methods for efficient residual error control (relaxation schemes that work well with irregular mesh intervals), and (3) adaptive mesh structures based on these error norms. The efficient interaction of these three key elements is necessary to obtain adaptive solution of the Navier-Stokes equations.

A follow-on research program is recommended which addresses development of the three key elements defined in the work reported herein and noted above. The development of these elements would occur simultaneously, utilizing a series of research computer programs of increasing complexity.

2

2.0 INTRODUCTION

The Navier-Stokes equations with continuity, energy and state equations are the accepted analytical model for fluids whose constituative properties are Newtonian. They apply to the flight envelope of most aircraft in the earth's atmosphere and to all steady and unsteady laminar and turbulent flow processes which influence the performance of these aircraft. The development of numerical techniques to model the Navier-Stokes equations has been revolutionary in recent years and the pace is accelerating.

The Navier-Stokes equations are always simplified to related but different partial differential equations (PDE). These simplified PDE systems are chosen to model the essential properties of the Navier-Stokes equations for the intended application. In the solution of many of these flows, it is difficult to sort out modeling errors from numerical errors. An obvious example is the use of the Reynolds averaged Navier-Stokes equations for turbulent flow.

Selecting appropriate PDE systems depends upon having an understanding of the PDE solution properties. These are defined through analytical and numerical methods. PDE modeling depends upon understanding the numerical results including distortions induced by numerical errors. It is important to control these numerical distortions to within tolerances that are consistent with the intended application. The cost to achieve a given level of accuracy is also important. The cost/benefit relation must be readily accessible, otherwise unrealistic levels of accuracy may be demanded without real benefits or insufficient accuracy may occur with misleading results.

The present effort is directed at the physics of smooth steady flows with interacting singularity regions such as shocks, boundary layers, free shear layers, flame fronts and contact surfaces. Existing solution techniques for the equations describing these flows are usually unable to control the length scales of the mesh in these singularity regions sufficiently to accurately resolve these flow features because they are inefficient at the necessary grid scales. As a consequence, computed results are of low accuracy.

3

Efficient numerical modeling of these equations with systems of algebraic equations for a grid is difficult because of residual errors in the solution process and truncation errors. Residual errors occur because of the Gibbs' effect (wiggles or high frequency oscillations in the solution) and the stiffness of the equations (acoustic, diffusive and convective stiffness). Stiffness is defined as slow convergence toward the target of zero residual errors. Truncation errors are due to the grid selected, the grid related algebraic equations solved, and the boundary and initial conditions - all used to approximate the field equations in an analysis domain. These problems are compounded by the grid requirements of singular flows; grid length scales are needed near singularities that vary by orders-of-magnitude from those required in regions of low gradients in flow properties.

Algorithms for numerical solution of the Navier-Stokes equations are sought which address simultaneously the requirements for

    a. grid related algebraic solution procedures for improved reduction of residual errors

    b. error monitors that efficiently assist the grid adjustment process and optimize the residuals relative to the truncation errors

    c. solution procedures which are less sensitive to mesh and permit grid nesting.

Adaptive grid control is the interaction of these elements to reduce numerical error. Manual and automatic processes can be used to implement adaptivity. A balance between computer code development time and computer code user complexity must be kept in mind.

The multi-level adaptive grid procedure[1] produces truncation error estimates as a by-product of the solution procedure which could be used as a resolution monitor. This procedure is thus especially attractive as an approach to the development of automatic PDE solvers which control numerical errors to a prescribed tolerance.

4

2.1   THE OBJECTIVES OF THE STUDY

The first goal of the research is the development of numerical error assessment methods for use as grid resolution monitors. The second goal is adaptive mesh generation methods to refine the grid locally where indicated by the resolution monitor. The third goal is to improve the efficiency of residual error control with non-uniform meshes. It is expected that the availability of this technology will provide significant improvement in the numerical solution of the PDE's of fluid mechanics. Substantial work is necessary before this will be possible. The objectives of the present work were to begin development of algorithms to define error norms and to begin development of multi-level adaptive grid techniques.[1] The present work is an initial exploratory investigation of resolution monitors, grid adjustment methods, and residual error control efficiency.

2.2   THE TECHNICAL APPROACH

Two overall strategies are being used to guide the development of resolution monitors and adaptive grid methods. The first strategy is to define as early as possible all of the elements necessary to the development of the desired technology and to address these simultaneously. The second is to use simple one-dimensional numerical "test beds" to define and develop the necessary technology elements. Once the technology elements are defined and developed, extension of the technology to test bed codes for 2-D and 3-D PDE's of fluid mechanics should be relatively straightforward. With this background, the error-norm adaptive grid technology can then be applied to codes for efficient solution of fluid flow analysis problems.

Specifically for the work reported herein the detailed technical approach was as follows:

1) The literature on error assessment and multi-grid methods was briefly reviewed. Error sources were identified, Section 3.1, and a brief mathematical description of these is presented in Sections 3.1.1 and 3.1.2. Control of numerical error with filtering and damping and the necessary interaction with error assessment methods are described in

Section 3.1.3. The problem of efficient residual error control is discussed in Section 3.1.4.

Conventional approaches to error assessment and control are discussed in Section 3.2. Three approaches were identified; the conventional certification process, Section 3.2.1, the engineering approaches, Section 3.2.2, and the error norm approaches, Section 3.2.3.

Four error norm approaches to numerical error assessment were identified. Conventional error norms are defined in Section 3.2.3.1. A Taylor series error monitor approach is described in Section 3.2.3.2. Variable order accuracy algorithms for error assessment are described in Section 3.2.3.3. Multi-grid error norms are then described in Section 3.2.3.4.

2) Solution of the one-dimensional potential equation was selected as a test bed to investigate error assessment and multi-grid methods, Section 4.0. Numerical solution of the potential equation using point relaxation is described in Section 4.1 and using point relaxation and a multi-grid procedure, in Section 4.2.

3) The test problem was solved using the point relaxation and the multi-grid scheme as described in Section 4.3.

4) The various error norms were evaluated as described in Section 4.4, and an adaptive mesh example is presented in Section 4.5.

5) Computed results were evaluated and are discussed in Section 5.0. Conclusions and recommendations for further work are suggested in Section 6.0 and 7.0.

6

3.0 NUMERICAL CONSIDERATIONS

3.1 TYPES OF ERROR SOURCES

The numerical methods for solving PDE's have two types of error sources: grid-related solution process (residual) errors and grid-placement related (truncation) errors. Explicit marching techniques (time or space) do not have residual errors unless there is an implicit equation imbedded in the marching scheme. Residual errors occur when implicit equations are solved by explicit marching techniques, specialized relaxation schemes or matrix inversion processes. Only ideal difference schemes have no truncation-error effects. Practical flow analysis tools are not ideal. Truncation-error and residual-error effects produce many curious phenomena which must be understood in order to develop reliable error norms. The error norms must be able to detect any spurious or peculiar numerical phenomena.

3.1.1 Mathematical Description

Let

$$LU = 0 \qquad\qquad 3.1.1\text{-}1$$

represent the PDE system of interest.

In discretized operator notation, equation 3.1.1-1 is

$$L^I U^I = T^I - R^I \qquad\qquad 3.1.1\text{-}2$$

where L^I is the discretization operator, U^I is related to the discretized dependent variable vector, and T^I is the local truncation error and R^I is the local residual error for each cell of the analysis domain. The grid structure index, I, is related to choices of the grid density distributions for each selected trial grid where in general the computational grid features coupled conformal grids with grid nesting in sub-regions. Ideally the grid adjustments are made in some pattern that tend toward a limiting grid configuration or 'goal grid.' Thus each unique grid shape is represented by an integer value of I. The 'goal grid' is assigned the index I_g, which is known once the numerical error has been constrained to the desired bound.

An ideal or perfect difference scheme for 3.1.1-2 is one in which the local truncation error does not contaminate the variables of interest, such as velocity, density, pressure, etc. Only the residual errors impact these variables. Thus, the user specifies exactly the locations in the geometry at which values of these variables are desired. With residual error control within adequate bounds, the accuracy of the result is insured within selected limits.

Non-ideal difference schemes are defined as those in which the local truncation error and residual errors simultaneously influence the value of the decoded variables. Except for specialized difference schemes for model problems, difference schemes for conventional applied analysis are non-ideal. Control of both error sources is addressed herein with emphasis on controlling the truncation error. This subject is closely related to the problem of proper grid adjustment from an initial state to the 'goal grid' state, with proper residual control during the grid-adjustment process.

3.1.2 Truncation (Grid Related) Errors

Truncation errors are due to the selection of the grid, the grid related algebraic equations, and the boundary and initial conditions which approximate the field equations of interest.

The local truncation error is formally defined as the magnitude that the left-hand side of (3.1.1-2) yields for each cell when the 'goal grid' solution is interpolated (restricted) to a trial grid difference equation minus the interpolated value of the left-hand side of (3.1.1-2) from the 'goal grid'. It is set at zero in conventional representations of (3.1.1-2) for all values of I. In the defect- and deferred-correction methods discussed in Sections 3.2.3.3 and 3.2.3.4, truncation error estimates are used to correct for truncation error effects. The right-hand side of equation (3.1.1-2) can also be a high-order accurate truncation error correction.

8

3.1.3 Filtering and Damping Spurious Numerical Waves

The linear wave equation is

$$u_y + u_z = 0$$

This equation exhibits many of the features of the convection terms of Navier-Stokes equations but it is simple enough that the powerful methods of linear analysis apply. Such analysis indicates that all the numerical methods that have been applied to model this equation have the following properties: Control of the phase errors, amplitude error and the Gibbs-effects errors[2] within selected accuracy bounds depends upon the proper grid density selection per period of propagation for wavelengths of interest and with properly designed Gibbs-effects filters. Truncation errors have an accumulative effect upon the accuracy.

Gibbs-effects errors are high frequency oscillations near the juncture of sharp changes in gradients. For the linear case, the Gibbs' error wavelength is about four, seven, sixteen and infinite (zero Gibbs effect) mesh intervals for eighth, fourth, second, and first order accuracy convective difference schemes, respectively. For nonlinear cases such as near shocks, the wave length of the Gibbs-effect error is about two mesh intervals for most schemes of all orders of accuracy above two. Wavelength smoothing[2] is very effective for controlling the amplitude of the Gibbs effect to within chosen bounds without introducing global damping. Low order accurate Gibbs-effects filters are especially useful for providing the global damping that is necessary for removing transient waves from certain types of relaxation processes. When properly tuned for the most effective use of the grid, the low order accurate filtering devices while serving to adequately damp the global waves may not provide sufficiently for the control of the Gibbs' oscillations within desired bounds. Wavelength filtering in addition to the global damping is well suited to the control of the Gibbs' oscillations within desired bounds because the smoothing can be localized as desired.

Intelligent use of smoothing is one of the central difficulties of modeling transient and steady state analysis involving mixed elliptic/hyperbolic equations. Where analytical solutions are unavailable, the error norms for analysis of required accuracy must account somehow for the phase, amplitude

and Gibbs-effects errors. The question whether the solution processes must be free of Gibbs-effects errors should be treated in future work?

Dissipative and non-dissipative convective difference schemes permit expansion shocks, artificial gross separation, etc. to form under certain conditions. Artificial diffusion is added to eradicate the expansion shocks. Tuning the artificial diffusion coefficients for peak accuracy is troublesome. The goal of the tuning process is that the artificial diffusion must decay globally and locally with mesh refinement so that the accuracy of the sonic line shape and position increase with mesh refinement. The error norm used must ensure this.

3.1.4 Residual Errors
The numerical modeling of the potential equation or of the Navier-Stokes equations leads to algebraic forms in which the propagation of signals is retarded as the grid density increases. This stiffness problem leads to inefficient reduction of residual errors among the simultaneous system of algebraic equations, often leading to exponential or power function decrease in convergence as the grid density increases. Typically diffusive stiffness is evident in potential flow codes. In Navier-Stokes codes, three stiffness problems can appear simultaneously or separately - acoustic, convective, or diffusive stiffness and can be aggravated by non-uniform grid. Any or all of these factors can undermine the convergence rate severely and can enlarge errors substantially. The error monitors must be designed to detect slow convergence or inefficient residual error control. For some error norms this is a severe requirement. When the local residual error is reduced to some fraction of the local truncation error, further reduction of the residual is not cost effective; determination of this fraction is a subject for further study.

3.2   ERROR ASSESSMENT AND CONTROL

Three approaches are used to assess the accuracy of PDE modeling. The first is to construct an error difference table with solutions on trial grids of various mesh densities and distributions. The second is the use of auxiliary information such as experimental data and related analytical solutions for various regions of the analysis domain, and the third is the use of the local truncation and local residual error estimates associated with suitable error norms and error bounds. These three are referred to as the conventional,

10

engineering (analogical) and the error-norm approaches to certifying the accuracy of PDE modeling. Direct numerical evidence of the accuracy of the PDE modeling results from the conventional and error-norm approaches. These methods have their origins in numerical analysis technology. In the engineering approach no attempt is made at achieving direct evidence. Inferential reasoning is predominately used. Discussions of this are given in the following sections.

3.2.1 Conventional Certification Process

The process of numerical error assessment with conventional PDE modeling techniques is the following.[3] A solution of finite difference equations (simultaneous system of algebraic equations) for a specific discretization of the analysis domain is generated for different choices of grid density and grid distribution in the analysis domain. It is common to use a sequence of grids of the same grid distribution that differ in grid count in each independent variable direction by factors of two -- 2, 4, 8, 16, 32, etc. The coarser grids can be generated by deleting every other point of the finer grids. The effects of the choice of grid distribution are examined by choosing sequences of grids which have different mesh distributions. The data from all of these solutions of the grid-related equations is organized by constructing an error difference table. Solution differences are posted in order of the coarse-to-fine grids for each grid sequence. The solution differences are generated by subtracting the values of adjoining pairs of grid solutions of the dependent variables at all physical locations in the analysis domain that correspond to the grid coordinates of a grid of a selected intermediate density. Interpolation is used to relate other grid solutions to these selected grid coordinates. As the grid density increases the differences should decay approximately* according to the formal order of accuracy for some selected mesh distribution. Iterative adjustment of the grid distribution and density is made until this type of error decay is realized. If this occurs, extrapolation may be used to solutions at infinite grid density and reliable estimates of the maximum global error may result.

---

*Error decay according to the formal order of accuracy is expected globally but not locally in regions of singularity.

The preceding process appears to work best on the modeling of parabolic and elliptic equations in smooth domains with smooth boundary conditions. For mixed elliptic/hyperbolic systems, erratic results may occur due to unresolved singularity regions and/or poor residual error control, and/or Gibbs' error effects.

A key feature of this method is that grid adjustments are made in some pattern that tends toward a limiting grid configuration. A way to think about this is to define a goal grid to which the selected grid sequences must evolve. The 'goal grid' is a grid upon which the solution is sought to some specified error bound. It should be understood that the 'goal grid' may not be unique because of grid initialization, grid generator, and grid-equation solver properties. It is assumed that adequate control of the residual error effects has been maintained in the process of assessing the truncation error effect. This is done by developing a sequence of _several_ _solutions_ on _each_ _grid_ _choice_ with various choices of constraints on the residual tolerances that are used to terminate the computations for each solution on that grid. Because of the need to assess the contamination by residual error, the 'goal grid' may not be the grid of greatest density but it will have the correct shape.

Conventional techniques for developing the data necessary to certify the accuracy of numerical modeling procedures are limited by the following factors:

1) Costs.

2) Because of (1) above, a very limited number of solutions and thus sparse information are usually available from which error estimates can be constructed.

3) Because grid adjustment to control the error within desired bounds is cumbersome or impractical, arriving at proper grid configurations in mesh density and distribution is also difficult or impractical.

4) Numerical error during grid refinement may vary erratically, not monotonically with grid density. Confusion as to grid adjustment needs can result.

12

5) The software is usually not available for conveniently constructing the error table. This means that the error assessment process is manpower intensive. These factors discourage development of the 'goal grid' solution. Without this, the accuracy of the result is unknown; the meaning of the result is undefined and useless unless appropriate external information (user experience) is applied to the result.

The certification process with conventional computer codes utilizes error information from many grid densities and grid geometries. This is a multi-grid process albeit a very cumbersome and inefficient one. For the present purposes this technology will be referred to as fixed grid (FG) even though it is not, when properly used for numerical error assessment. It is called FG because that is the manner in which it is used in applications; the error term associated with each number in the output is set to zero and this is often ignored in the use of the numbers from the output.

3.2.2 Engineering Approaches

Judgement in engineering applications as to what grid should be selected for numerically modeling a PDE system is often based upon an exterior body of knowledge[3] rather than direct numerical evidence. For example, boundary-layer analysis can be performed with finite difference and related analysis tools. Mesh refinement studies and conventional error norms can be used to define the accuracy and grid-choice relationships. Similar studies can be performed on free shear layer and inviscid model problems with analytical solutions to establish the accuracy and grid-choice relationships. The various component features of the physics of the PDE system can be studied in this manner. The selection of the trial grid for the PDE system of engineering interest can be made upon the basis of the physics that is expected in each flow region of the analysis domain. The grid selection in the various flow regions of the analysis domain can reflect the desired accuracy that is required locally and globally for the purposes of the analysis. Interpretation of the results of numerically modelled PDE systems involves qualitative aspects of the solution. Inspection is used to insure that solution features such as wall shear stress, wall boundary layer, free shear layer, inviscid structure, or shock structure characteristics occur

13

where they are expected. The success of this approach depends on the knowledge and skill of the analyst and the time allotted for the analysis. Important physical processes may be inadvertently ignored because numerical errors mask solution properties. For example, artificial diffusion can be interpreted as turbulent diffusion.

Another approach to grid selection is used in engineering applications as well and sometimes augments the above approach. It involves the comparisons of computed and experimentally measured flow properties. Grid and local and global numerical smoothing adjustments are used to generate favorable agreement between the computed and measured flow properties. Where experimental data is available, this approach is preferred to those that are described above and it encourages the use of analysis for predictive purposes where favorable agreement occurs.

In engineering approaches, direct numerical evidence is not used to understand the nature of the numerical properties; rather inferential and analogical reasoning are used.

3.2.3 Error Norm Approaches

Four possible methods are considered here. The first method is a brief review of conventional error norms; the second is the use of truncated Taylor series expansions for an error monitor; the third is the use of variable order accuracy algorithms; and the fourth is the multi-grid approach. These are discussed below.

3.2.3.1 Conventional Error Norms

Standard error norms[4] include:

$$E_1 = [\; \Sigma |(\phi^I - \phi^{II})|\;]/N \qquad\qquad 3.2.3.1-1$$

$$E_2 = [\Sigma(\phi^I - \phi^{II})^2 / (\phi^I)^2]^{1/2} \qquad\qquad 3.2.3.1-2$$

$$E_{max} = [\,|(\phi^I - \phi^{II}) /\phi^I |\,]_{max} \qquad\qquad 3.2.3.1-3$$

ϕ = amplitude

14

where ϕ^I is the dependent variable of the _analytical solution_ restricted to the coordinate location of grid point I. N is the number of grid points. ϕ^{I1} is the discretized solution on grid I. The sums denote component sums in 2-D and 3-D situations. E_1, E_2, and E_{max} are known as the average error, the root-mean-square (rms) error and the maximum global error, respectively. The E_{max} norm is best applied to non-singular problems (no shocks, shear layers, or geometry discontinuities) with smooth boundary conditions although it can be used if the regions of steep gradients are excluded. E_1 and E_2 are used for singular perturbation problems including the steep gradient regions. The use of these definitions as written depends upon knowing ϕ^I which is not available for cases of general interest. However, modified forms of these relations may be considered.

For example, equations 3.2.3.1-1 through 3.2.3.1-3 can be given by:

$$E_1^{I1,I2} = [\ \Sigma |(\phi^{I2} - \phi^{I1})| G(Z) \ ]/N \qquad\qquad 3.2.3.1-4$$

$$E_2^{I1,I2} = [\Sigma((\phi^{I2} - \phi^{I1})^2/(\phi^{I2})^2)]^{1/2} \qquad\qquad 3.2.3.1-5$$

$$E_{max}^{I1,I2} = [G(Z)|(\phi^{I2} - \phi^{I1}) /\phi|^{I2}]_{max} \qquad\qquad 3.2.3.1-6$$

where ϕ^{I2} is any of ϕ^{I1+1}, ϕ^{I1+2}, ... ϕ^{Ig}. ϕ^{I2} is also regarded a higher order accurate solution on grid I1. G(Z) is a weighting factor which may be used to exclude regions in the analysis domain where the local truncation error estimates exceed a selected threshold value. N is the number of cells in the summation. These error norms should be of general use for understanding the role of residual and truncation errors, especially when used with the error norms discussed below.

There are error estimators in addition to the ones listed above which should be considered in any application of interest. For example, certain components of PDE systems require that kinetic energy, mean vorticity, total pressure, entropy, mass, etc. should be conserved. Discretized forms of these integral relations could be constructed which are relevant to the application of interest.

15

3.2.3.2 Taylor Series Error Monitor

The idea of using truncated Taylor series expansions for an error monitor has been explored and conclusions about the cost effectiveness of such a development are summarized as follows. Consider a simple harmonic function such as the y=sin x. From calculus, the derivatives of all orders exist. The odd-order derivatives vanish when the modulus of the even-order derivatives are maximum. At the least, pairs of odd-order and even-order derivatives would have to be approximated by finite difference expressions to prevent spurious decay of higher-order terms in any proposed error monitor. The second requirement is that, in regions of the grid with long wavelength variations of a dependent variables of interest, it must establish how many pairs of odd and even orders are required to certify the numerical accuracy of the PDE modeling. The third requirement is that, since high frequency oscillations (two mesh interval limit) can excite two mesh interval oscillation on all discretized derivative of the order of two and above, this information must be used somehow to sort Gibbs errors, geometric discontinuities, etc. While the Taylor series error monitor idea is intriguing, it has conceptual and implementation problems. The next section describes a related but perhaps better approach to error assessment.

3.2.3.3 Variable Order Accuracy Algorithms for Numerical Error Assessment*

Rather than using only mesh refinement to assess numerical error, it is conceptually reasonable to define numerical algorithms of variable order of accuracy from which direct error estimates emerge for a given grid. A way to think about this is to define a sequence of higher order accurate discretized solutions on the same grid each of which satisfy a certain smoothness property. The higher order accurate solutions on the grid are regarded as the trial analytical or reference solutions. The lowest order accurate solution is regarded as the approximation. The error estimate is performed with conventional error norms. The error norms of Section 3.2.3.1 are slightly modified for error assessment by using higher order accurate solution data in place of the I2 finer grid data. Iteration can be used to determine how high

---

*   Defect- and deferred-correction schemes are closely related because error estimates are used to improve the efficiency of residual error control. Both methods are multigrid methods.

16

the order of accuracy must go for reliable error estimates. Grid adjustments are needed to provide the highest order accurate scheme with sufficient grid to meet desired accuracy bounds.

To implement the above process, a convergent variable order of accuracy algorithm approximating the PDE system of interest must be available. For the boundary layer equations, Wornom[5] presents an approach. Forester[2] suggests a method for mixed hyperbolic/parabolic PDE systems using odd-degree splines although other basis functions can be used. The order of accuracy of this scheme is selected simply by choosing the appropriate coefficient matrix that is associated with the desired accuracy. With this method, orders of accuracy six, ten, fourteen, nineteen, etc. are possible and they are activated by an input control function. Interpolation is used to initialize successive solution processes of higher accuracy.

Lindberg[6], Pereyra[7] and Stetter[8] have developed an approach which is related to the one described above but in which certain simplifications are implemented. Basically Lindberg uses a low order accurate approximation to the PDE system with a non-zero right-hand-side term that is lagged in the iteration process. This perturbation operator is a high-order-accurate discretization (usually fourth order) of the PDE system. The data for the perturbation operator is derived from the low order of accuracy discrete equation system solution. The perturbation equation is repeatedly solved until some convergence criterion is satisfied. The output of the perturbation equation is a correction parameter. It is added to the low order of accuracy solution to yield a fourth order accurate solution at convergence. Error estimates are produced with conventional error norms by using the high-order-accurate solution as an exact representation of the PDE system. The low order accurate result represents the approximate solution. Lindberg presents many examples of the efficiency of this defect-correction procedure to reduce residual and truncation errors. Success is not universal with hyperbolic problems, however, when some smoothness property is violated. It may be inferred from Lindberg's data that if sufficient smoothing is applied to regions of rapid change in gradient, convergent results are achieved. To make Lindberg's scheme useful for hyperbolic systems, empirical studies would have to be performed to develop criteria for how local the smoothing must be constrained so that the global errors are definable. See Section 5.3 for related discussion.

17

The approaches of references (1-8) presume that some sort of mesh refinement process toward the 'goal grid' is used. The accuracy of these error estimators improves dramatically as the accuracy moves toward the one percent error range. They are useful guides for grid refinement when errors are larger than ten percent but are not precise in the predicted magnitude. These approaches are promising for modeling mixed parabolic/elliptical/hyperbolic systems of equations but are difficult to implement when grid nesting is required.

Another approach to defect-correction has been proposed by Brandt[9]. This approach suggests variable order of accuracy, nested grids, enhancement of residual control efficiency and the efficient generation of an error term that may be useful for numerical error assessment. This approach has been called the multigrid method but it is misnamed since all numerical assessment and control schemes are multigrid.* Many variations of this methodology are possible. Most examples of this approach[1,8,10] are for residual control efficiencies near theoretical limits with uniform grid intervals. Irregular grids (nested grids) have yet to be widely addressed in this method.

3.2.3.4 Multi-Grid Error Norms

Modifications are suggested in Section 3.2.3.1 to conventional error norms for assessing numerical error schemes. This is applicable to the FAS-MG (Full Approximation Storage-Multi-Grid) scheme with one exception. The solution data at each grid level must be saved before finer grid levels are invoked in the multi-level solution process. This approach insures that the targets of residual and truncation errors are zero in the output for the various levels of grid. If this is not done, solution errors may appear on coarser grids when in fact none exist.

The FAS-MG scheme estimates local truncation error by interacting coarse and fine grid solution data. Brandt suggests that the weighted integral

$$\bar{E}_T = \int G(z)|T(z)|dz \qquad\qquad 3.2.3.4\text{-}1$$

---

* Brandt's approach could be called defect-correction multi-grid or Tau multi-grid, TMG.

18

is a measure of global error level, E_T, where $G(z)$ is either zero or unity. $G(z)$ represents a weighting to exclude singularities in the analysis domain. $T(z)$ is the local truncation error. The discussion in paragraph 3.1.4 suggests that additional error norms should be considered for the control of residual errors. For example, relationships such as

$$\bar{E}_R = \int |R(z)| \, dz \qquad \qquad 3.2.3.4\text{-}2$$
$$\bar{E}_{RT} = \int |R(z)|/|T(z)| \, dz \qquad \qquad 3.2.3.4\text{-}3$$

may be suggested.

These error norms can be readily generalized for more space dimensions. $R(z)$ and $T(z)$ are normalized by some suitable reference quantity so that they cannot exceed unity during the solution process. Singularities in the PDE modeling are detected by $T(z)$ of the order of unity.

4.0 NUMERICAL ANALYSIS AND RESULTS

With reference to the technical approach, Section 2.2, solution of a one-dimensional potential equation was selected as a test bed to evaluate error assessment and multi-grid methods. Solution of the one-dimensional potential equation was selected because of its simplicity, only a single dependent variable. The equation was solved using a point relaxation scheme alone and then a multi-gridded point relaxation scheme.

A test problem, a channel flow with a constriction, was selected because analytical solutions are available for comparisons with the numerical solutions. The test flow was solved for a range of mesh densities and distributions and the more promising error assessment techniques were evaluated. The test problem was also solved with a multi-gridded point relaxation scheme to understand and evaluate the characteristics of the multi-grid scheme. A semi-self-adaptive mesh scheme was briefly investigated.

4.1   SOLUTION OF THE 1-D POTENTIAL EQUATION

The discretized 3-D full-potential equation for steady incompressible flow is restricted to a 1-D analysis tool by deleting the K and L indicies in the Ref. 10 formulation. The total velocity can be computed in many ways. One formulation[10] yields values of the total velocity in which the truncation errors in the velocity potential do not contaminate the computation of the total velocity.

The forms of the 1-D continuity equation for the purposes of the present study are in terms of the primitive velocity component, W, and the velocity potential, ϕ. They are given by

$$(WA)_z = 0 \qquad\qquad 4.1\text{-}1$$
$$[\phi_z A]_z = 0 \qquad\qquad 4.1\text{-}2$$
$$W = \phi_z \qquad\qquad 4.1\text{-}3$$

where A is the channel cross section.

The transformed discretized forms of these equation are given by

$$[((W)(D))_{M+\frac{1}{2}} - ((W)(D))_{M-\frac{1}{2}}]^I = T_M^I - R_M^I \qquad \text{4.1-4}$$

$$[(\phi_{M+1} - \phi_M)(C_{M+\frac{1}{2}}) - (\phi_M - \phi_{M-1})(C_{M-\frac{1}{2}})]^I = T_M^I - R_M^I \qquad \text{4.1-5}$$

$$W_{M+\frac{1}{2}}^I = [(\phi_{M+\frac{1}{2}} - \phi_M)(C_{M+\frac{1}{2}}/D_{M+\frac{1}{2}})]^I \qquad \text{4.1-6}$$

I   = grid level index, I = 1 coarsest grid, two cells in domain range of
            zero and unity for Z/L

$C_{M+\frac{1}{2}}$ = $(2)(D_{M+\frac{1}{2}})^2/(VL_M + VL_{M+1})$

$D_{M+\frac{1}{2}}$ = $1 - Y_{M+\frac{1}{2}}$

$Y_{M+\frac{1}{2}}$ = 1   Z less than zero

$Y_{M+\frac{1}{2}}$ = Y(z) $0 \leq Z \leq L$ cubic functions

$Y_{M+\frac{1}{2}}$ = 1   Z greater than 1

VL_M = $(D_{M-\frac{1}{2}} + D_{M+\frac{1}{2}})(Y_{M+\frac{1}{2}} - Y_{M-\frac{1}{2}})/2$

R_M = residual error due to inexact solution process

M   = the grid index of cell centers

M   = 1, dummy cell for boundary condition data

M   = 2, first cell in analysis domain

M1   = M_{max} + 1, last cell in analysis domain

M2 $= M_{max} + 2$, dummy cell for boundary condition data

ϕ_{M2} $= We \, (VL_{M1} + VL_{M2})/(D_{M1+\frac{1}{2}})/2 + O_{M1}$ boundary value

ϕ_1 $= \phi_2 - We \, (VL_1 + VL_2)/(D_{2-\frac{1}{2}})/2$ boundary value

$M+\frac{1}{2}, M-\frac{1}{2}$ = grid index of cell face of cell M, $Z_{M+\frac{1}{2}}$, $Z_{M-\frac{1}{2}}$

M_{max} = grid index of cell face on cell M

We = velocity at entrance of the 1-D channel

Given We, $D_{M+\frac{1}{2}}$ for $2 \leq M \leq M1$, and R_M for $2 \leq M \leq M1$, equation 4.1-4 is solved exactly for $W_{M+\frac{1}{2}}$ by marching from M=2 to M1. The analytical solution to equation 4.1-1 is recovered by equation 4.1-4 at any selected z coordinates if R_M is identically zero during the marching process (round-off error effects are ignored for practical purposes.) With T_M^I and R_M^I selected equal to zero, equation 4.1-4 is regarded as a perfect or ideal difference scheme. Equation 4.1-5 is regarded a perfect difference scheme in terms of W_M since equation 4.1-4 results from combining equations 4.1-5 and 4.1-6.

Relaxation methods can be used to approximate equation 4.1-5. Two relaxation equations are

$$\phi_M^+ = [[(\phi_{M-1}^a)(C_{M-\frac{1}{2}}) + (\phi_{M+1}^O)(C_{M+\frac{1}{2}})]/(C_{m-\frac{1}{2}} + C_{m+\frac{1}{2}})]^I$$

a = o, Richardson scheme   4.1-7a

a = + , Liebmann scheme   4.1-7b

ϕ_M^+ = updated

ϕ_M^O = old value

Note that R_m is set to zero when deriving equaions 4.1-7 by the manipulation of 4.1-5.

The FG method of solving equation 4.1-2 is defined by iterating equation 4.1-7a or 4.1-7b until some test on the residual show that this process should be terminated.

4.2   SOLUTION OF THE 1-D POTENTIAL EQUATION WITH MULTI-GRID

The FAS-MG scheme is more elaborate. It is defined as follows. Equations 4.1-7a and 4.1-7b are modified by inserting a term, RS_M, into the numerator so that they read

$$(\phi_M^+) = [(\phi_{M-1}^a)(C_{M-\frac{1}{2}}) + (\phi_{M+1}^o)(C_{M+\frac{1}{2}}) + RS_M]^I/(C_{M+\frac{1}{2}} + C_{M-\frac{1}{2}})^I$$

a = o, Richardson scheme   4.2-1a

a = +, Liebmann scheme   4.2-1b

$$RS_M^I = [(I_{Ig}^I(\phi_{M+1}^{Ig}) - I_{Ig}^I(\phi_M^{Ig}))(C_{M+\frac{1}{2}})^I - (I_{Ig}^I(\phi_M^{Ig}) - I_{Ig}^I(\phi_{M-1}^{Ig}))(C_{M-\frac{1}{2}})^I]$$

$$- I_{Ig}^I[(\phi_{M+1}-\phi_M)(C_{M+\frac{1}{2}}) - (\phi_M-\phi_{M-1})(C_{M-\frac{1}{2}})]^{Ig} \qquad\qquad 4.2-1c$$

RS_M^I is the local truncation error estimated on grid I relative to grid Ig on which RS_M^{Ig} is set to zero. I_{Ig}^I is the restriction operator for the conversion of data on grid Ig to a usable form on grid I. The subscripts in equation 4.2-1c refer to grid I. The process of generating ϕ_M^{Ig} data that is necessary to use equation 4.2-1c is provided in an excellent form by Brandt (Ref. 8). The variant of this process adapted here (see diagram 1) is to start on the coarsest grid (Level 1) with equation 4.1-7b. When the mean residual tolerance of 10^{-4} or lower (see below) is satisfied, standard

linear interpolation of the velocity potential to the next finer grid level is implemented. Equation 4.1-7b is iterated on this grid (Level 2) until a minimum number of iterations (1, 2, 4, 8, 16, 32 were used) are completed. Further iterations are required if the ratio of the new and old residuals, the eigenvalue, is less than some amount - .82 was used based upon trial-and-error experience. The rate of residual error reduction is slowing if .82 is exceeded. When this occurs, it is time to switch to the next coarser grid (Level 1). This means that the ϕ_M^2 are interpolated from the Level 2 grid to the Level 1 grid and Equation 4.2-1b is introduced. RS_M^1 is estimated from Equation 4.2-1c with Ig replaced by 2. A converged solution to a low residual tolerance is produced on Level 1. Velocity potential data for Level 2 again must be interpolated from existing data at Levels 1 and 2. For this purpose, Brandt's prolongation* operator is used. The details of this equation are provided later in this discussion. It may take several Level 1 and Level 2 cycles before a low residual tolerance is achieved on Level 2. Once convergence on Level 2 is achieved, prolongation to Level 3 is used with standard linear interpolation of the velocity potential on Level 2. Equation 4.1-7b is iterated on Level 3 until the minimum number of iterations are performed or until the critical eigenvalue is exceeded. Restriction to Level 2 provides an estimate of RS_M^2 from Level 3 using the Equation 4.2-1c with Ig replaced by 3. Level 2 is iterated with this value until the solution is stalled. Restriction to Level 1 provides a corrected estimate of RS_M^1. Cycling between Levels 1, 2, and 3 continues until Level 3 residual tolerances are satisfied. Level 4 is then used. This process can go on indefinitely, but it is usually terminated at Level 5. See Diagram 1 for a flow chart description of the FAS-MG scheme that is used.

The RM_M^I term is composed of two components -- the residual and the local relative truncation estimate. At the finest grid yet arrived at during the multi-level solution process, these elements are of equal and of opposite sign so that the target of RS_M^I is exactly zero. In regions of the coarse grid solutions where the truncation error estimate should be zero, it is not zero but it has a magnitude proportional to the residual error on the finest grid yet arrived at. Its actual magnitude depends on how many grid levels it is

---

*Prolongation is defined as interpolation to a finer grid.

Brandt's FAS—MG Scheme (Modified with Error Control on Residual)

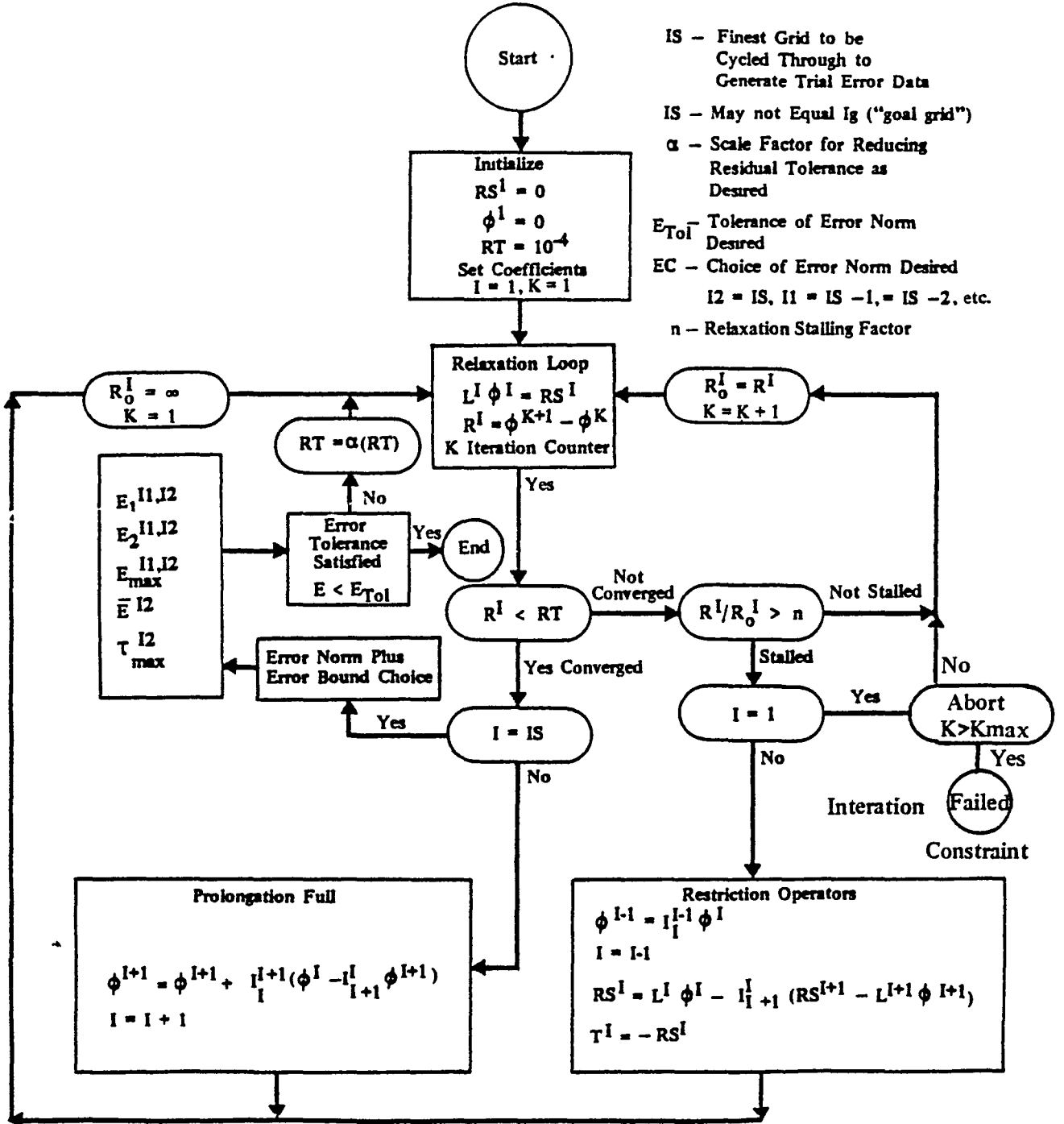Coarest-to-Finest Grid Approach to $L\phi = 0$

Start

IS — Finest Grid to be Cycled Through to Generate Trial Error Data

IS — May not Equal Ig ("goal grid")

α — Scale Factor for Reducing Residual Tolerance as Desired

E_{Tol} — Tolerance of Error Norm Desired

EC — Choice of Error Norm Desired

I2 = IS, I1 = IS −1, = IS −2, etc.

n — Relaxation Stalling Factor

Initialize
$RS^I = 0$
$\phi^I = 0$
$RT = 10^{-4}$
Set Coefficients
$I = 1, K = 1$

$R_0^I = \infty$
$K = 1$

Relaxation Loop
$L^I \phi^I = RS^I$
$R^I = \phi^{K+1} - \phi^K$
K Iteration Counter

$R_0^I = R^I$
$K = K + 1$

$RT = \alpha(RT)$

No

$E_1^{I1,I2}$
$E_2^{I1,I2}$
$E_{max}^{I1,I2}$
$\bar{E}^{I2}$
τ_{max}^{I2}

Error Tolerance Satisfied
$E < E_{Tol}$

Yes

End

Yes

$R^I < RT$

Not Converged

$R^I/R_0^I > n$

Not Stalled

Error Norm Plus Error Bound Choice

Yes Converged

Stalled

No

I = 1

Yes

Abort
K>Kmax

Yes

No

Yes

$I = IS$

No

Interation

Failed

Constraint

Prolongation Full

$\phi^{I+1} = \phi^{I+1} + I_I^{I+1}(\phi^I - I_{I+1}^I \phi^{I+1})$

$I = I + 1$

Restriction Operators

$\phi^{I-1} = I_I^{I-1} \phi^I$

$I = I-1$

$RS^I = L^I \phi^I - I_{I+1}^I (RS^{I+1} - L^{I+1} \phi^{I+1})$

$T^I = -RS^I$

DIAGRAM 1

25

removed from the finest grid yet arrived at. A rule-of-thumb is that the residual error of the finest grid yet arrived at is about doubled each time the grid intervals are doubled.

For the present studies, two approaches to the selection of residual tolerances are examined. The residual tolerance can be chosen either for the coarsest grid or the finest grid. In the former method, the coarsest grid residual tolerance is reduced by a factor between two to four each time the grid size is doubled. Alternatively, if the finest grid residual tolerance is chosen, it can be applied to all grid levels. Both methods have been used. The latter method is recommended for simplicity in the use of the modified error assessment formulas of paragraph 3.2.3 which are discussed in Section 4.4.

4.3   THE TEST PROBLEM

The 1-D test problem involves an analytical geometry of a straight channel with a cubic function for a constriction that reverts either abruptly step-wise or smoothly to a straight channel. Figure 1 shows the channel section shape distribution with respect to the flow direction. Figure 2 snows the analytical solution restricted to 65 grid coordinates (64 cells) with the grid intervals constant. Eleven trial fine-grid sets were used to examine the 1-D potential solution properties for a) grid with uniform mesh intervals, b) grid with uniform mesh intervals in the region of cross sectional area variation but with a stretch factor of two in the straight sections, and c) grids with uniform mesh intervals in the straight sections but with a stretch factor of .80, .85, .90, .95, 1.0, 1.05, 1.1, 1.15, and 1.2 in the constricted region where the finest grid is near the abrupt enlargement of the channel cross sectional area for stretch factors less than unity. The total number of grid intervals for each set of trial grids are 4, 8, 16, 32, and 64, where the number of grid intervals in the constriction region are respectively 2, 4, 8, 16, and 32. FG and MG methods have been applied to generate solutions, shown in Figure 2, by the solid line for the finest grid. Also shown in Figure 2 is the FG and MG solutions with very high residual error tolerances. Using point

relaxation* and sweeping the grid in the flow direction, MG yields a maximum global error** of less than 4% in the equivalent*** of twenty-five sweeps of the 64 node grid, whereas FG requires over one thousand sweeps of the 64 node grid to achieve the same accuracy. The maximum error occurs at the geometric discontinuity. Increasing the accuracy by an order of magnitude requires less than a factor of three increase in the work for the MG and the FG. The process of solving the problem to greater accuracy can be continued until the maximum global error satisfies desired constraints up to round-off error effects. The boundary conditions are imposed both on the FG and MG as set mass rates of equal magnitude at the entrance and exit cross sections.

Figure 4 shows the truncation error spectrum for the peak values of the local truncation error asymptotically approach nearly the same values including T-extrapolation, on the next-to-the-finest grid solution. The magnitude of these terms are substantial near the discontinuity and, because they form the right-hand side of the cell-wise flux balance equations, induce large errors in the total velocity profiles that are shown in Figure 3. The coarse-to-fine grid correction equation of Brandt very effectively interpolates the Poisson type solutions on coarser grids so that the coarser grid solutions mimic the finer grid solutions. Standard interpolation (prolongation),

$$\phi^{I+1}_{new} = I^{I+1}_I (\phi^I_{new})$$

cannot account on the next finer grid, I+1, for the fact that the right-hand side term is significant in the coarser grid solutions. For this reason, standard interpolation is not useful and must be replaced by a more elaborate interpolation. Brandt recommends (for prolongation)

$$\phi^{I+1}_{new} = I^{I+1}_I (\phi^I_{new} - I^I_{I+1} \phi^{I+1}_{old}) + \phi^{I+1}_{old}$$

---

* Both Richardson and Liebmann point relaxation were used. As expected, the efficiency of FG and MG are improved with Liebmann relaxation. Conclusions about the asymptotic efficiency with mesh refinement holds irrespective of the form of the relaxation used here. All of the displayed results are with Liebmann relaxation.

** The global error is defined by equation 3.2.3.1-3.

*** See the discussion in Section 5.2 for a definition of equivalent sweeps.

where I_{I+1}^{I} is the fine-to-coarse grid interpolation operator and I_{I}^{I+1} is the coarse-to-fine grid interpolation operator. This expression functions well as illustrated in Figure 5. Linear interpolation is used for these operators with weightings of 1/4 and 3/4 for I_{I}^{I+1} and weightings of 1/2 and 1/2 for I_{I+1}^{I}. These weightings are derived directly from the geometric relationship between the coordinates of the cell centers of the two adjacent grid levels whose cell faces coincide at every other cell face. No modification of this weighting is used for stretched grid cases whose principle effect is to retard the convergence rate by up to one-third for cases with stretch factors of .80 and 1.2.

4.4   ERROR NORM EVALUATION

The utility of the error norms of paragraphs 3.2.3.1 and 3.2.3.4 is examined in this section. Errors in the computed velocity are studied with the use of the maximum global error estimator and average and maximum truncation error estimators. It is expected that similar conclusions would be reached if other error estimators of paragraph 3.2.3.1 were used.

The unmodified (analytical reference) and the modified (finer grid reference) maximum global error norms (E_{max}, $E_{max}^{I1,I2}$) of Section 3.2.3.1 and the error norms of Section 3.2.3.4 have been applied to a number of cases of 1-D incompressible channel flow that have smooth and abrupt cross sectional area changes. A new error norm is defined and is used as well. The results for these error norms are summarized as follows.

To illustrate the properties of E_{max} and $E_{max1}^{I1,I2}$, an output station is chosen for which the grid levels -- 2, 4, 8, 16, and 32 cells in the transition region of the channel geometry. In all cases, the location is selected nearest the minimum channel cross section where the largest errors in velocity reside. E_{max} increases in size as the grid size and/or the residual tolerances grow. However, this nice behavior does not occur with $E_{max}^{I1,I2}$. $E_{max}^{I1,I2}$ is not unique since the output from the various grid levels, I2, is used for the reference solution.

28

Let I2 equal grid levels 2, 3, 4, and 5 to examine the maximum estimated global error for the coarsest grid, I1=1. $E_{max}^{I1,I2}$ values increase in size as the reference grid level and/or the finest grid residual tolerances grow. $E_{max}^{I1,I2}$ values are a measure of relative error between solutions at different grid levels and as such may have a different sign and level than E_{max}. Furthermore, $E_{max}^{I1,I2}$ values define the error in the <u>reference grid solution,</u> I2, rather than in the approximate solution, I1, under examination. This conclusion is predicated upon having the residual tolerance for the approximate solution within an error bound that is about the same magnitude as the reference grid which causes a <u>more accurate</u> coarse grid solution than that of the finer reference grid solutions. This result holds strictly only for a perfect difference scheme. For nonperfect difference schemes, local truncation error will likely dominate the coarse grid solutions. However, it is possible that peculiar local truncation error may produce smaller real error in coarse grid solutions. Therefore, it is necessary to use additional information to determine if the error indicator $E_{max}^{I1,I2}$ is a measure of coarser grid error. One method of determining this is to examine the behavior of $E_{max}^{I1,I2}$ as the residual tolerance is reduced. For a nonperfect difference scheme, $E_{max}^{I1,I2}$ should reach a fixed value for some range of residual tolerance. If so, the $E_{max}^{I1,I2}$ indicator is measuring the coarser grid error. Otherwise, residual error effects are dominant.

The behavior of $E_{max}^{I1,I2}$ is illustrated for $E_{max}^{3,4}$, $E_{,max}^{3,5}$ and $E_{max}^{1,5}$. $E_{max}^{3,4}$ predicts the error in the level 4 solution to about thirty percent accuracy of the true error. $E_{max}^{3,5}$ predicts the error in the level 5 solution to about a five percent accuracy of the true error on level 5. $E_{max}^{1,5}$ predicts the error in the level 5 solution to about a one-half of one percent accuracy of the true error. These statistics are for a residual error of 10^{-6} at all grid levels. This residual tolerance reflects about a one tenth of one percent true error range for the level 5 solution. For the ten percent true error range of level 5 solutions, the precision is reliable to better than an order of magnitude. This provides a useful guide for grid density adjustments.

The behavior of $E_{max}^{I1,I2}$ is spurious when the residual is controlled on each grid level to yield the true error of the same magnitude on each grid level. Brandt recommends residual error control in this fashion which renders $E_{max}^{I1,I2}$ useless for ideal difference , schemes. For this reason and because nonideal difference schemes may locally, in certain cases, behave like an ideal difference scheme, it is suggested that it is better to control the residual to the same level on each grid level even though this guideline may not yield peak computatonal efficiency exclusive of the error assessment costs.

Application of Equation 3.2.3.4-1 with G(z) set equal to unity yields the average value of the local truncation error. The average and maximum values of the local truncation error are examined for utility in error assessment. When scaled by the channel cross section, these quantities are converted into average and maximum velocity perturbations, respectively. The scale factors are the average and the minimum channel cross sectional areas, respectively. These velocity perturbations have been correlated to the maximum global error in the fluid velocity for various grid levels that contain the nonzero R.H.S. on all but the finest grid. The average velocity perturbation predicts conservatively the right order of magnitude that the MG generated maximum velocity must be corrected by in order to estimate the error in the MG output. This result applies to smooth and discontinuous channel shapes with uniform grid intervals. The use of the maximum value of the local truncation error appears to be best reserved for locating discontinuities in the solution since it tends to overestimate the solution error levels in all grid levels. This error estimator will be especially useful to identify regions in the analysis where the mesh interval is too large irrespective of how coarse the grid is in the neighborhood of discontinuity in dependent variables such as temperature, pressure, tangential velocity, etc. For the immediate future this error estimtor has application to all existing flow codes. The installation of the FAS-MG scheme in these codes would be useful just for that purpose alone. Considerable cost saving could be realized by using this method of guiding the grid adjustments.

Only one exact method of evaluating the maximum and local global error has been found for the perfect difference scheme. The sums of the same-sign local

truncation error are converted into velocity perturbations by the use of Equation 4.1-4. The sign content of these terms oscillate to produce non-smooth corrections. Starting at the edge of the analysis domain, these sums are added one-by-one. This velocity is called the modified exact velocity. At each point where the sign change occurs in the velocity perturbation, the error between the grid solution and the modified exact velocity is computed and saved. All of these errors are sorted until the largest is found. The largest value is the maximum global error on the finest grid level to within round-off error effects which means that it has extreme accuracy. Roughly the error is bounded by one part in ten to the ten on the CDC CYBER 175 computer.

4.5   ADAPTIVE GRID EXAMPLE

In this section, uses of the local truncation error estimates for grid adjustment are discussed. A simple example of semi-adaptive grid refinement is shown in Figure 6 in which grid compression toward the region of high local truncation error is used. Iterative grid compression is continued until a condition of the maximum normalized local truncation error is less than .08. Semi-adaptive grid compression is implemented in the interval $0 \leq Z/L \leq 1$ by iteratively decreasing the grid stretch factor from an initial value of 1.2 in steps of .05. As expected, the tolerance on the maximum local truncation error is not satisifed as long as an exact step-wise discontinuity is enforced at a Z/L equal to unity. With a cubic transition function in the interval $31/32 \leq Z/L \leq 32/32$ which has a slope continuity with the remaining channel geomtry, local truncation error reduction results with grid refinement. Figure 6 shows the results of the analytical solution and solution with a grid contracted toward Z/L equal to unity. Over an order of magnitude reduction in the local truncation is readily achieved with a contraction ratio of .85. The lower the magnitude selected for the stopping criteria, the more grid is compressed into the region of the abrupt geomtry change. Eventually this approach starves the remaining domain of the analysis of sufficient mesh to satisfy the selected maximum local truncation error tolerance. Therefore a preferred strategy involves sub-dividing the region of small length scale, $31/32 \leq Z/L \leq 32/32$, with a uniform grid of varying

number of grid points. It is easy to implement. It is regarded also as semi-adaptive. A 'fully' adaptive strategy requires labeling each cell of a trial grid with a special flag that designates cells with a local truncation error that exceeds a selected threshold value. Cells so flagged may be sub-divided by nesting compressed grids or by uniform interval grid embedding. It is expected that the rapid grid-interval changes may produce a growth in local truncation error in that region. If this occurs, criteria must be developed for the control of the rate of the grid interval varations or the meaning of the truncation error reassessed. 'Fully' adaptive MG strategy only requires that iterative work to reduce the truncation error be applied to the flagged cells. This approach may be more efficient, 'fully' adaptive and more computer programming intensive than the semi-adaptive strategies. This approach appears to be practical to program for machine computations for multi-dimensional numerical analysis.

32

5.0 DISCUSSION

5.1 ERROR ASSESSMENT

For the test problem, local normalized truncation error estimates of the order of unity seem to indicate the region in which grid adjustment (mesh density or distribution) should occur or the region in which the geometric representation of the boundary of the analysis domain may need modification. The local truncation error estimates in themselves cannot distinguish the cause of large local error or whether the results of the analysis are adversely affected. Therefore additional information must be associated with the local truncation error estimates to make them useful. The behavior of the solution in high gradient regions in terms of second derivatives of certain dependent variables may be useful in developing criteria which distinguish the source of truncation error from Gibbs' error. Together with the residual data, each region having large truncation error can be sorted as to the cause of the large truncation error. Criteria for choosing the G weighting in the error norms of 3.2.3.1 and 3.2.3.4 perhaps can be developed from this basis. See Section 5.3 for further discussion of this point.

At a geometric discontinuity, the sign of the local truncation error oscillates at the highest possible frequency of two mesh intervals for an ideal difference scheme. This produces a cancellation of the local truncation error in the velocity solution.

It is hypothesized that nonideal difference schemes will exhibit two-mesh-interval sign oscillations in the local truncation error estimates only at singularities or at locations which have grid-related problems. Otherwise the local truncation error estimates will persist at longer wavelengths. It is hypothesized that sums of the same-sign local truncation errors are significant to estimating the maximum global error for nonideal difference schemes. Useful sums may or may not include the regions of large local truncation error depending on the purpose for the error norm. It is

hypothesized that the magnitude and the rate change of the local truncation error may have use for an error norm where grid juncture in composite grids occur or where rapid variations in the dependent variables occur.

Residual errors and maximum global errors were observed to be directly linked. This was examined by computing the discrete continuity balance (local mass balance) on each cell. By dividing the local mass balance by the local channel cross sectional area, a delta velocity results which, added to the local velocity, is the correction necessary to remove the local residual error. The maximum global error was reduced to round-off error (below ten to the minus ten) when the residual velocity correction was applied successively from the entrance region point-by-point through the grid to the exit region. Alternatively the maximum global error can be computed directly from the sum of the residuals of the same sign divided by the channel cross section at which the sign in the residual changes. Control of residual errors is all important for satisfying desired global error bounds. It is hypothesized that the local residual error should be constrained to some value smaller than the local truncation error on the grid which is next to the 'goal grid.'

5.2   MULTI-GRID

The form of MG that was used for the computations involves a nonzero right-hand side term. With this formulation the discretized continuity equation has a mass source right-hand side term which is constructed from the estimate of the local truncation error. Fine grid velocity potential data are interpolated (restricted) to coarse-grid continuity balances to obtain estimates of the local truncation error where global integral is zero for mass conservation. Total velocity output that is decoded from solutions of these coarse-grid Poisson-type equations are not directly useful (with an academic exception). This is a key point about MG output: the total velocity output on the coarsest grids may be contaminated with large truncation errors. This point is illustrated in Figure 3 for three grid levels. Note that the results near the geometric discontinuity are always badly in error. In the coarsest grid the local truncation error from the geomtric discontinuity contaminates the total velocities at three cell faces where the solution is developed. The

34

extent of the contamination is reduced dramatically as the grid is refined but it is only eliminated on the finest grid level where it is exactly zero by choice. Any other choice for the finest grid solution would generate worse results than that shown; the maximum global error would be larger near the discontinuity than occurs in the present example. Therefore the truncation error extrapolation[9] cannot be inserted at the finest grid level, only at next to the finest grid levels. As shown in Reference 9, it can be used as a method for accelerating solution convergence or for generating still finer grid solutions (finer than 64 cell cases in the present example) at lower cost. Alternatively, a finest grid selection of 32 cells could be used with T-extrapolation to get the solution that is shown in Figure 2.

Standard interpolation fails to be useful for prolongating coarser grid MG solutions to finer grid levels. Brandt's FAS-MG formulation is effective for this purpose. Estimates of the local truncation error are a direct consequence of the FAS-MG process. The maximum value has utility for identifying discontinuities. The mean value is a useful guideline of the maximum global error.

It appears desirable to modify conventional applied analysis codes with the Brandt FAS scheme so that local truncation error estimates are a routine output. This will aid in quickly identifying regions of the analysis domain where truncation error problems exist. An optimum MG scheme is not the issue for the short term. It is desirable to reduce the labor involved in determining where in an analysis domain serious numerical error problems are occurring. It may also be feasible to develop error norms that exploit the local trunation error estimates of MG so that conventional, semi-adaptive and adaptive composite grid technology can achieve high efficiency.

The grid generation and the PDE solution processes must be drawn together to be effective. Composite grid technology should be encouraged. Composite grids refer to coupled conformal grids in which nested grids, grid overlays, and discontinuous grids are permitted by the analysis approach.

Multi-Grid Computer Cost Overhead

The efficiency of residual error control in terms of computer overhead cost for the MG approach was briefly examined. Under the test problem Section 4.3, the word "equivalent" sweep was utilized to compare the number of sweeps in an MG scheme with FG sweeps. "Equivalent" sweep is defined as follows. Neglecting the overhead for the use of the restriction and prolongation operations for generating RS_M^1 and O_M^2 estimates, the number of iterations on each grid level can be equated to one sweep on the finest grid. Thus 16, 8, 4, and 2 are "equivalent" sweeps on grid levels 1, 2, 3, and 4 respectively relative to level 5 grid. The ratio of the "equivalent" sweeps and FG sweeps is not identical with the ratio of $(CPU)_{MG}$ to $(CPU)_{FG}$. To achieve parity between these measures of work, a correction factor must be empirically generated which corrects the "equivalent" sweeps for the overhead of the MG process. This factor is computer and computer code dependent and it is not identical with operation counts. No effort has been made to study the optimum magnitude of this cost correction factor. For the present application, this correction factor is about the same magnitude as the cost to sweep the relaxation equation on the finest grid. No optimization of the coding was attempted to reduce the size of this factor. Therefore the $(CPU)_{MG}/(CPU)_{FG}$ ratio is approximated by $(sweeps)_{MG}/(sweeps)_{FG}$ times two. A preferred definition of "equivalent" is one that includes this factor.

Control of the contamination of the total velocity output is correlated with the computer work expended in solving the grid equations. The data shows that the residual error control efficiency increasingly favors MG over FG as the number of grid points is increased. To illustrate this, computations were performed as follows. Level 5 grid equations were iterated until a selected maximum global error was achieved. The same problem was repeated four more times for the maximum global error level using MG. Each problem was constrained between two limits of grid level in the MG processes. The grid levels are: level 4 - level 5, level 3 - level 5, level 2 - level 5, and level 1 - level 5. The $(CPU)_{MG}/(CPU)_{FG}$ ratio was estimated by the above formula for each problem. It decreased with the extension of the grid level separation. The same result was found if the study was performed in the

36

opposite order; namely, (level 1)$_{FG}$ and (level 1)$_{MG}$, (level 2)$_{FG}$ and (level 1 - level 2)$_{MG}$, (level 3)$_{FG}$ and (level 1 - level 3)$_{MG}$, (level 4)$_{FG}$ and (level 1 - level 4)$_{MG}$, and (level 5)$_{FG}$ and (level 1 - level 5)$_{MG}$. This result is in keeping with Brandt's results. For a simple elliptic problem, this establishes one type advantage of MG over FG procedures: MG is asymptotically more efficient than the FG strategy in controlling residual error. Hence the number of grid points that can be considered in an analysis with MG is greater than FG for a given computer budget. The potential for control of truncation error is thus greater with MG than FG strategy for nonideal difference schemes.

5.3   CONTROL OF THE LENGTH SCALES OF STEEP GRADIENT REGIONS

The practical utility of the error norms listed in paragraphs 3.2.3.1 and 3.2.3.4 requires quantitative relationships between error norms and such parameters as wall skin friction, separation and reattachment points, stagnation point location and properties, growth rates of shear layer thickness, and the length scale of the resolution of shock waves relative to shear layers with which they interact.

Special attention should be devoted to developing the criteria for the control of the length scale of shock waves and stagnation points. One interesting recent hypothesis[12,13,14] is that shock waves and stagnation points often need not be resolved to their true physical length scale. They only need to be resolved to length scales of the order-of-magnitude of the key or diffusive and boundary regions of the flow field with which they interact. The development of quantitative information on the length scale of the large local truncation error regions (shock, flame fronts, chemical species fronts, and stagnation regions) relative to the diffusive and and boundary regions with which they interact is needed. The laminar shock/boundary layer interaction problem[12,13,14] would be especially suitable for such studies. For inviscid computations, singularity length scales must be an input parameter.

The error norms of equations 3.2.3.1-4, 3.2.3.1-6, 3.2.3.4-1, and 3.2.3.4-3 have a parameter which must be set to zero in the neighborhood of the

singularity regions. The purpose of this parameter is to allow the local truncation error to be large relative to the smooth parts of the flow field. The detection of these regions is essential. How this can be accomplished is a key problem for future work.

Ideas for detecting these regions can be drawn from mathematical and physical features of singularities. For example, shock waves have associated jump conditions which characterize the upstream and downstream states in the inviscid flow. As the grid refinement process develops, periodic checks can be made for the cells that have large second derivatives of these dependent variables. Empirical tuning will probably be necessary to define the amount of guard mesh around the steep gradient regions that is necessary for limiting the grid refinement process.

6.0 CONCLUSIONS

An initial exploratory investigation has been completed toward the development of error norms for use as resolution monitors, multi-level adaptive grid techniques, and residual error control efficiency for the numerical solution of the PDE's of fluid mechanics. Key results are that multi-grid schemes are promising as a basis for developing solution resolution monitors, adaptive grid techniques, and improved residual error control efficiency. This work suggests that multi-grid technology is conceptually straightforward to apply to conventional elliptic equation computer codes. Further work is required to develop convenient error norms for the local error quantities to guide adaptive mesh adjustment with efficient residual error control.

7.0 RECOMMENDATIONS

Various research codes can now be written, based on this initial study, to use as vehicles to develop the technology further towards the ultimate goal of (semi-)automatic numerical error control in solving the compressible, rotational viscous 3-D equations of fluid flow. Reliable numerical error monitors for residual and truncation error assessment with efficient control methods in conjunction with nested, composite grids should be addressed. The following research codes are recommended, with the specific study items listed for each of the codes that examine the utility of E_1, E_2, E_{Max}, E_T, E_R, E_{RT}, T_{Max} and R_{Max}.

3-D Multigrid Potential Code

A three-dimensional multi-grid code, modeling the full potential equation for shockless and shock containing flows, is needed as a test bed for studying error norms that relate the maximum global error to the integrals of the local multigrid truncation error estimates. With this code, items can be studied such as:

    a.   Correlation of the maximum global error with different residual tolerances

    b.   Convergence criteria for residual tolerance based on maximum local truncation error estimates at each grid level or the finest grid level

    c.   Examine ways to best include steep gradient regions in error norm computations.

1-D Multi-Grid Euler Code

A one-dimensional multi-grid code, modeling the Euler equations for analytically generated channel shapes is needed to study shockless and shock containing flows to develop technology features, such as:

    a.   The residual control efficiency as affected by the choice of relaxation schemes

40

b.   The inherent behavior of schemes to remove the acoustic stiffness as a stability constraint or modifications needed to achieve the infinite speed of sound in low Mach number flow regions

c.   Error norm candidates based on integrals of the local truncation error estimate and their relationship to the maximum global error

d.   The inherent capability of multi-grid schemes to remove diffusive stiffness from the stability constraints on fine grid levels

e.   Examine approaches to the treatment of steep gradient regions in the error norm computations.

2-D Multi-Grid Euler/Navier-Stokes Code

A two-dimensional multi-grid code, modeling the Euler and Navier-Stokes equations for shockless and shock containing flows is needed to begin applying the technology features of error control multi-grid schemes to selected problems such as laminar boundary layer and shock/boundary-layer interactions on a flat plate.

Adaptive Embedded Multi-Grid Technology

The above studies with the various research codes will examine criteria for the local multi-grid truncation error estimates that can be utilized for labeling cells in which grid nesting is necessary. Recommendations can then be made for work tasks to further develop adaptive grid embedding in the 1-D Potential, Euler and Navier-Stokes codes and similarly for the 2-D and 3-D codes. The design of each of the recommended computer codes should be carried out with the goal of flexible grid nesting capability given top priority.

9.0 REFERENCES

1. Brandt, A., Dendy, J. E., and Ruppel, Hans: The Multi-Grid Method for Semi-Implicit Hydrodynamics Codes, J. of Comput. Physics, 34, 348-370, 1980.

2. Forester, C. K.: Higher Order Monotonic Convective Difference Schemes, J. of Computational Physics, 23, 1977, pp. 1-22.

3. Forester, C. K.: Advantages of Multi-Grid Methods for Certifying the Accuracy of PDE Modeling, Multigrid Symposium, October 20-21, 1981, NASA-Ames Research Center.

4. Issacson, E. and Keller, H. B.: Analysis of Numerical Methods, John Wiley and Sons, Inc., 1966.

5. Wornom, J. F.: Critical Study of Higher Order Numerical Methods for Solving the Boundary-Layer Equations, NASA Tech. paper 1302, NASA-Langley Research Center, November 1978.

6. Lindberg, Bengt: Error Estimates and Iterative Improvements for the Numerical Solution of Operator Equations, Dept. of Computer Science, U. of Illinois at Urbana-Champaign U.S. Air Force Office of Scientific Research, Bolling AFB, D.C. 20332, AFPSR-75-2854, July 1976.

7. Pereyra, Victor: Highly Accurate Numerical Solution of Caselinear Elliptic Boundary-Value Problems in Two Dimensions, Math. of Comput., 24, October 1970.

8. Stetter, Hans J.: The Defect Correction Principle and Discretization Methods, Number. Math. 29, 425-443, 1978.

9. Brandt, Achi: Multi-Level Adaptive Techniques (MLAT) for Singular Perturbation Problems, in Numerical Analysis of Singular Perturbation Problems, P.W. Hemker and J.J.H. Miller, eds., Academic Press, London, 1979.

10. Forester, C. K.: Numerical Prediction of Compressible Potential Flow for Arbitrary Geometries, Winter Annual Meeting, ASME, December 1979. Also accepted for publication in J. of Fluids Engineering.

11. Brandt, Achi: Multigrid Solvers for Non-Elliptic and Singular-Perturbation Steady-State Problems, Computers and Fluids, to appear.

12. Murphy, John: Unpublished study NASA-Ames Research Center on the grid requirements to resolve shock/laminary boundary layer interactions, May 1982; to be published.

13. Peery, K. M.: Unpublished Boeing study on grid requirements to resolve shock/boundary layer interactions, March 1982.

14. Messina, N. A.: A Computation Investigation of Shock Waves, Laminar Boundary Layers and Their Mutual Interaction, Ph.D. Thesis, Princeton University, 1977.
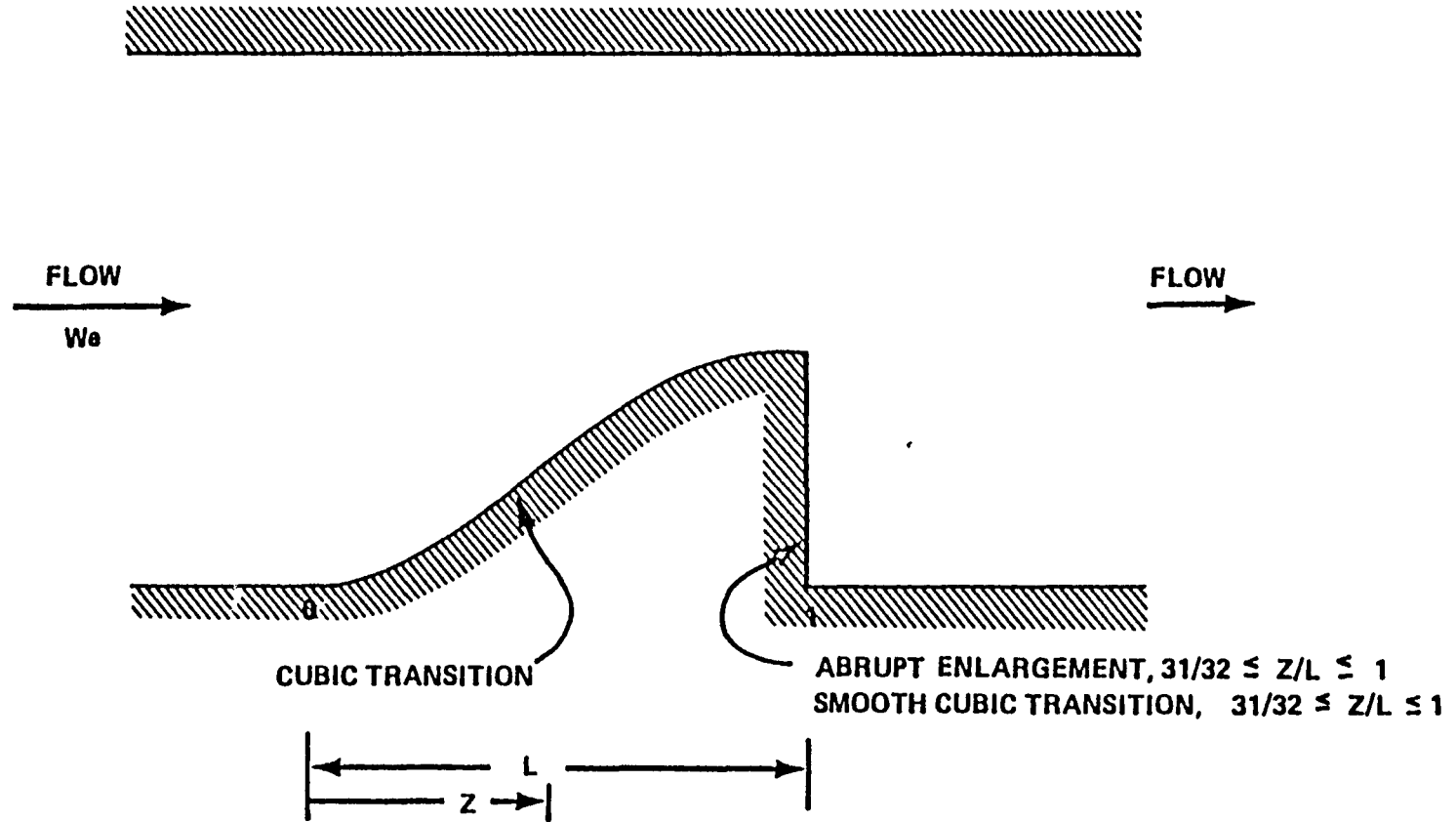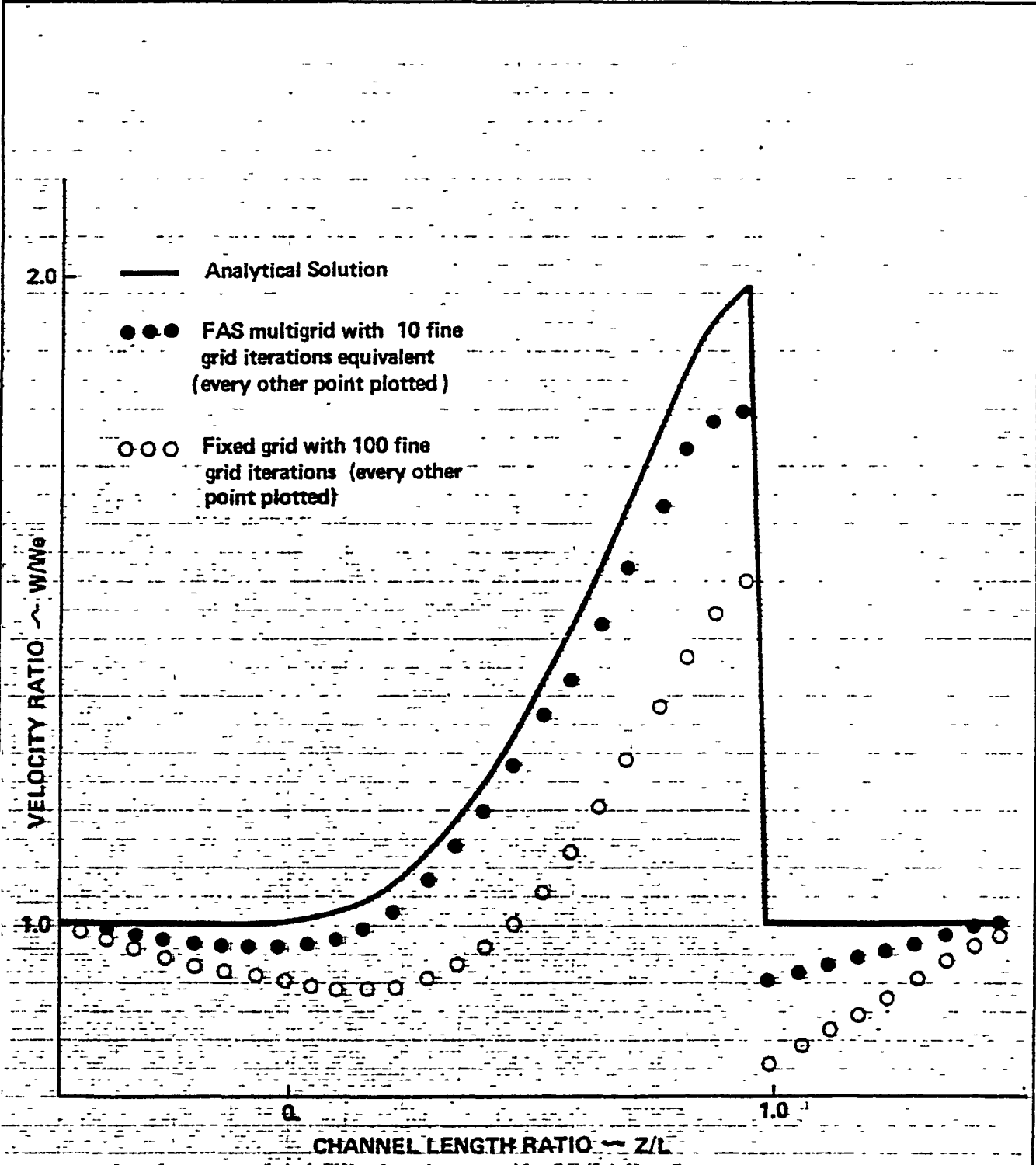
Figure 1. One-Dimensional Incompressible Channel Flow

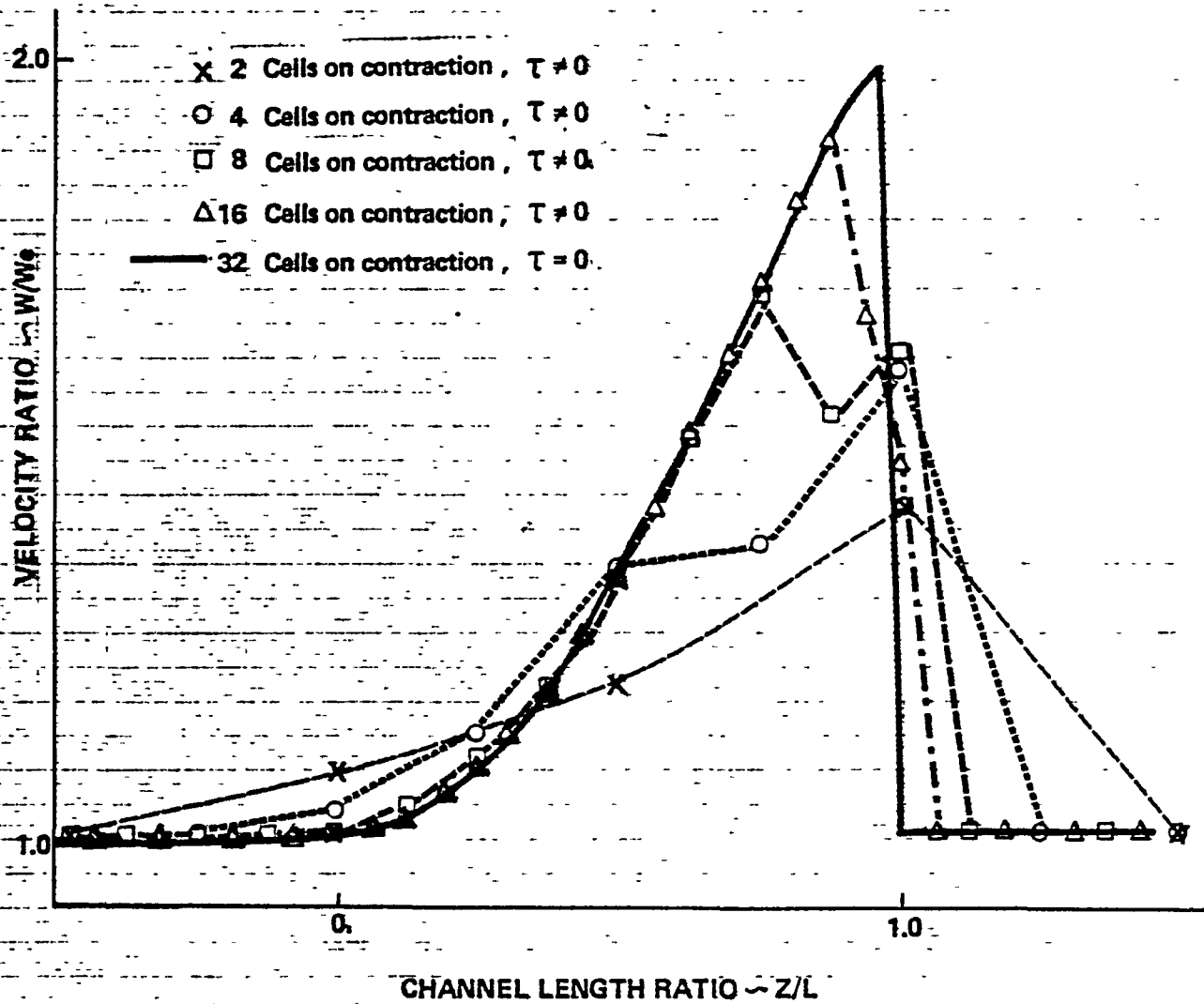Figure 2. Residual Error Effects on Fixed Grid and Multigrid Solutions

Figure 3. Truncation Error Effects on Intermediate Grid Level Solutions

Legend (on chart):
- ✕ 2 Cells on contraction, $\tau \neq 0$
- ○ 4 Cells on contraction, $\tau \neq 0$
- □ 8 Cells on contraction, $\tau \neq 0$
- △ 16 Cells on contraction, $\tau \neq 0$
- ── 32 Cells on contraction, $\tau = 0$

Y-axis: VELOCITY RATIO — W/W_e (2.0, 1.0)

X-axis: CHANNEL LENGTH RATIO — Z/L (0, 1.0)
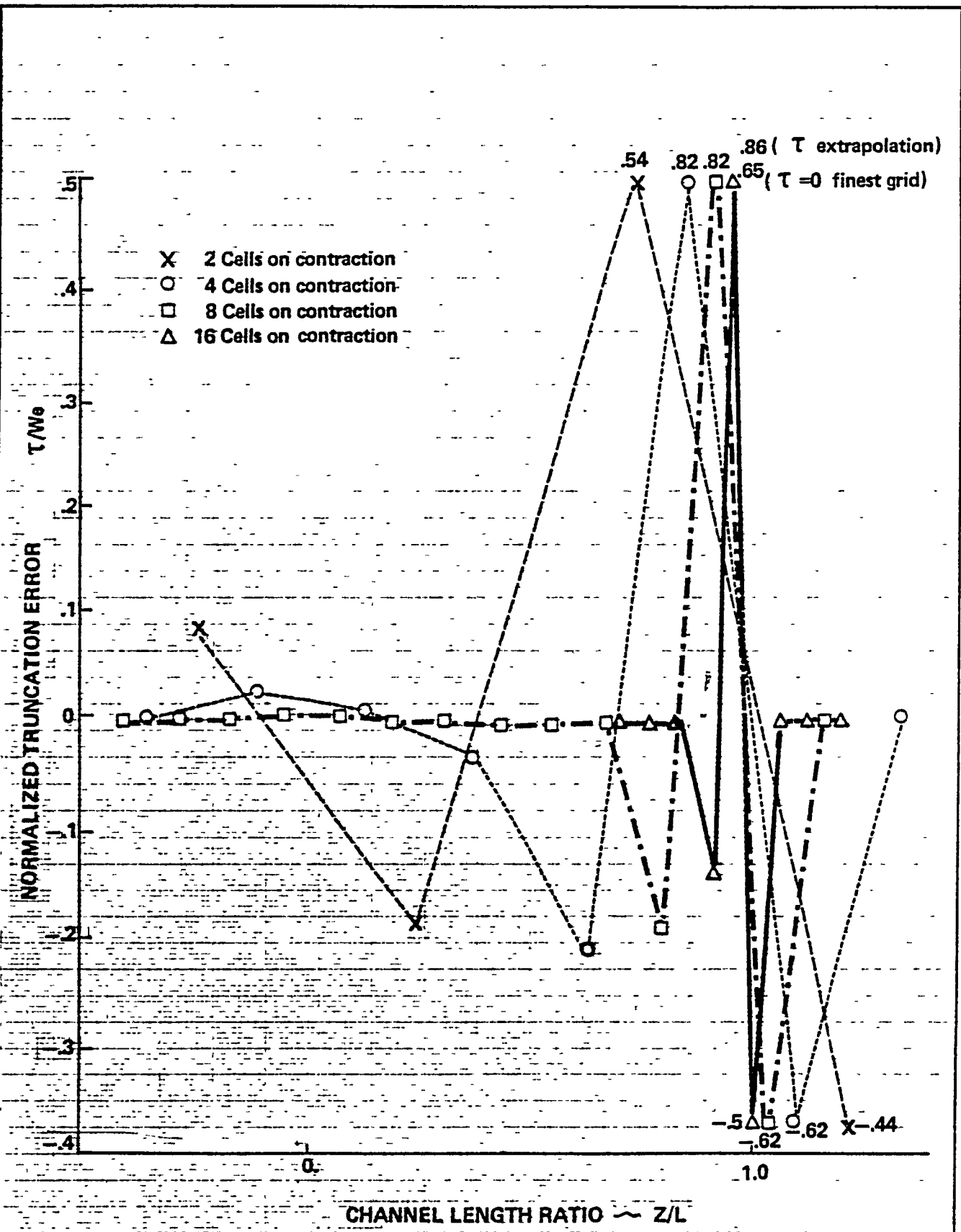
Figure 4. — Truncation Error Spectrum as a Function of Grid Density.

Figure 5. Why Brandt's Coarse-to-Fine Grid Correction Equation is Needed

Legend (shown within figure):
- ☐ 8 Cells on contraction, standard interpolation
- ⊙ 8 Cells on contraction, Brandt's FAS interpolation
- ●●● 32 Cells on contraction, Standard interpolation
- ○○○ 32 Cells on contraction, Brandt's FAS interpolation
- —— Solution exact for 32 cells on the contraction section

Y-axis: VELOCITY RATIO ~W/W(R)
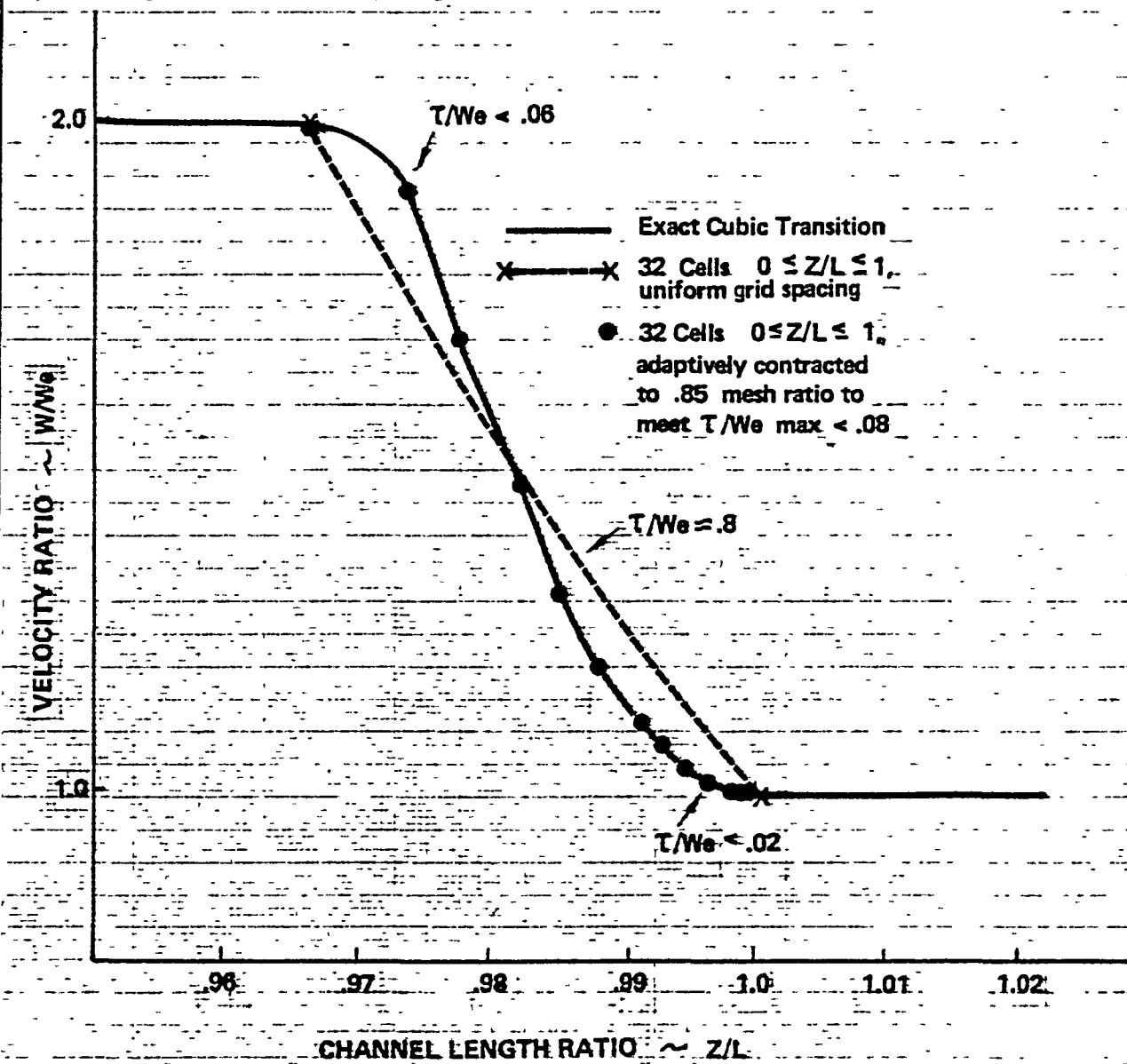
X-axis: CHANNEL LENGTH RATIO ~Z/L

Figure 6. Adaptive Grid Control to Selected Truncation Error Tolerance

End of Document